# The relationship between knee motion and articular surface geometry

# Chapter 27

# The Relationship Between Knee Motion and Articular Surface Geometry

R. Huiskes, L. Blankevoort.

## Introduction

The motion characteristics of the human knee joint are of a complex, three-dimensional nature. Its actual motion patterns depend partly on the anatomical arrangements of the bony and ligamentous constraints, which dictate its passive freedom of motion characteristics, and partly on muscle activity during a particular function, which determine the actual motion patterns within the passive motion envelope. Hence, understanding the relationships between anatomical and structural properties on the one hand, and passive motion characteristics on the other, is important for the study of knee-joint biomechanics in general. Information about these relationships is, of course, also important in a clinical sense, for the development of diagnostic and reconstructive procedures in knee-joint traumatology, and for the design of artificial joints. The diagnosis of ligament injury, for example, is partly based on the manual assessment of three-dimensional joint-laxity characteristics, relative to the non-injured knee. Hence, a pure consideration of passive motion feasibilities (Markolf et al. 1976; Fukubayashi et al. 1982; Edixhoven et al. 1989).

As a mechanical system, the tibial-femoral joint can be characterized schematically as in Figure 1. Joint motion is an effect of internal and external forces. The external forces are effects of muscles, gravity and accelerations, and applied directly to the bones outside the articular area. The internal forces are generated by articular contacts

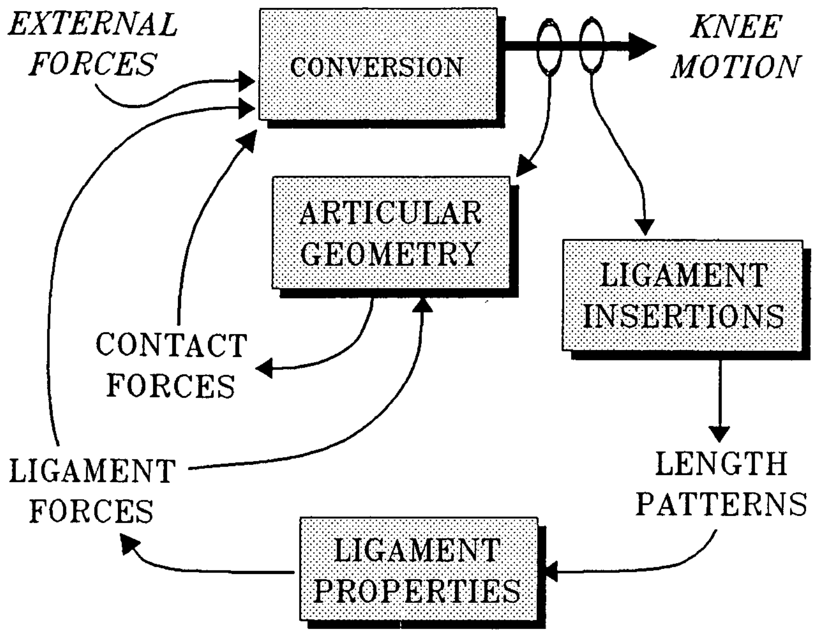


FIGURE 1: Schematic model of interactions between knee-joint structures and passive motion characteristics.

and ligamentous constraints, and depend, via articular geometry and ligament properties, on the relative motions of the joint. Hence, two feedback loops couple the output of the system to the input, including a cross-link between the loops by an additional mechanical coupling mechanism between ligaments and articular-contacts through the articular geometry.

The experimental and analytical studies performed to obtain a better understanding of the mechanical behavior of the knee joint can be put into perspective relative to the schematic model of Figure 1. These include measurements of particular properties such as ligament structure and geometry (Danylchuk 1975), ligament stress/strain behavior (Butler et al. 1986; Woo et al. 1983), ligament insertion geometry (Van Dijk 1983), articular geometry (Huiskes et al. 1985; Kurosawa et al. 1985), and mechanical properties of articular cartilage (Mow et al. 1982). Relationships studied, for example, were those between motion and ligament length patterns (van Dijk et al. 1979; Huiskes et al. 1984; Hefzy and Grood 1986), between motion and ligament forces (Ahmed et al. 1987), and between motion and contact forces (Ahmed and Burke 1983). Other studies considered the direct relationships between external forces and motions (Blankevoort et al. 1988). In many studies, the effects of properties or parameters of the feed-back loops on the force/motion relationships were evaluated, most predominantly relative to ligament properties or ligament forces, as for example by sequentially cutting ligaments (Butler et al. 1980), or by measuring ligament forces under variable external joint loads (Ahmed et al. 1987).

The purpose of this chapter is firstly to investigate the role of the articular geometry in the passive motion characteristics of the knee-joint, and its interactions with the ligaments. For this purpose, a three-dimensional computer-simulation model is applied. Several of these mathematical models have been reported in the literature (Crowninshield et al. 1976; Wismans et al. 1980; Andriacchi et al 1983; Blankevoort and Huiskes 1987a; Essinger et al. 1989). Although initially relatively crude and sometimes oversimplified, recent developments in computer capabilities, modelling capacities and data on mechanical properties of the knee-joint elements have caused the models to mature into realistic simulation tools. The second goal, therefore, of this chapter is to demonstrate the applicability and usefulness of mathematical (total joint) models for the development of a better understanding of knee-joint mechanics.

# Methods

## The Knee Joint Model

The three-dimensional mathematical knee-joint model used in the present investigation originates from Wismans et al. (1980). It features arbitrarily shaped 3-D articular surfaces, an arbitrary number of nonlinear line elements representing the ligaments, an arbitrary system of 3-D external loads, and it describes the complete 3-D relative motions between tibia and femur. It was later extended to account for deformable articular surfaces and for ligament/bone interactions (Blankevoort et al. 1990). Because of their mechanically complex nature and their secondary role in constraining motions (Blankevoort et al. 1984), the menisci are not included in the model as yet.

The computer procedure solves a set of six nonlinear equilibrium equations, using the Newton-Raphson method:

$$\mathbf{f}_e + \mathbf{f}_r + \mathbf{f}_l + \mathbf{f}_c = 0, \tag{1}$$

and

$$\mathbf{m}_e + \mathbf{m}_r + \mathbf{m}_l + \mathbf{m}_c = 0 \tag{2}$$

where $\mathbf{f}_e$ and $\mathbf{m}_e$ represent the system of externally applied forces and moments, $\mathbf{f}_r$ and $\mathbf{m}_r$ the constraint forces and moments which react to the prescribed degrees of freedom, $\mathbf{f}_l$ and $\mathbf{m}_l$ represent the total ligament loads, and $\mathbf{f}_c$ and $\mathbf{m}_c$ the total articular contact loads.

All forces and moments are assumed to act on the femur and are expressed relative to the space-fixed coordinate system of the tibia. The displacements of the femur are described relative to the (space-fixed) coordinate system of the tibia by a translation vector $\mathbf{a}$ and the Euler rotation matrix $\mathbf{R}$:

$$\mathbf{p} = \mathbf{a} + \mathbf{R}.\hat{\mathbf{p}} \, , \tag{3}$$

where $\mathbf{p}$ is the location vector of an arbitrary point of the femur expressed relative to the space-fixed system, and $\hat{\mathbf{p}}$ the location vector of the same point in the femoral body-fixed system. The rotation convention is similar to the one proposed by Grood and Suntay (1983).

In using the model, one or more of the relative displacements (3 translations and 3 rotations) can be prescribed, for which appropriate kinematic constraint forces are introduced in the equations (Blankevoort et al. 1990).

The ligament force $\mathbf{f}$ in a line-element in the body-fixed system is expressed by

$$\mathbf{f} = -f(L)\mathbf{v} \, , \tag{4}$$

where $\mathbf{v}$ is the unit vector pointing along the line of action of the element, and L its actual length. In accordance with Wismans (1980), f(L) is taken as

$$\begin{aligned} f &= \tfrac{1}{4}k\varepsilon^2/\varepsilon_1 && \text{when } 0 \le \varepsilon \le 2\varepsilon_1 \, , \\ f &= k(\varepsilon - \varepsilon_1) && \text{when } \varepsilon > 2\varepsilon_1 \, , \\ f &= 0 && \text{when } \varepsilon < 0 \, , \end{aligned} \tag{5}$$

where $\varepsilon$ is the actual strain in the ligament line element, $\varepsilon_1$ a strain constant and k a stiffness constant. This implies zero force for negative (compressive) strains, nonlinear force/strain behavior for strains below $2\varepsilon_1$, and linear force/strain behavior for strains beyond $2\varepsilon_1$ (Figure 2). The actual strain $\varepsilon$ is determined from the actual length L of the line element and its zero-load length $L_0$:

$$\varepsilon = (L - L_0)/L_0 \, . \tag{6}$$

The actual length L follows directly from the kinematic variables (3) and the insertion locations. The parameters k, $\varepsilon_1$, $L_0$ and the insertion locations of the line elements are to be determined experimentally.

To describe articular contact, a linear first-order model for contact

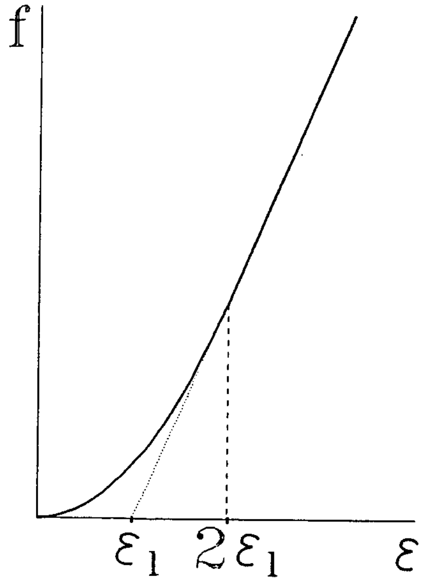


FIGURE 2: Assumed force/strain behavior of the ligament line-elements in the model (see formulas in the text).

flexibility is used (Kalker 1985). The subchondral bone is assumed as being rigid and the articular cartilage as a thin layer of linear-elastic material. The contact region is assumed to be large relative to the cartilage thickness and articular friction is neglected. The relationship between surface compression ($\sigma(\mathbf{p})$) and indentation ($\mathbf{u}(\mathbf{p})$) at a particular point **p** at the surface can then be described by

$$\sigma = \frac{S}{b} u \,, \qquad (7)$$

when linearity is assumed, or

$$\sigma = -S\ln(1 - u/b) \,, \qquad (8)$$

when nonlinear strain-hardening is taken into account. S is a stiffness parameter depending on the elastic modulus and the Poisson's ratio, and b is the thickness of the cartilage layer.

The contact force is determined by numerical integration of $\sigma(\mathbf{p})$ over the surface, for which the indentation variable $u(\mathbf{p})$, perpendicular to the surface, is coupled to the kinematic parameters (3), using the surface normal vector for orientation (Blankevoort et al. 1990). The stiffness parameter S, the cartilage thickness b and the geometry of the articular surface must be determined experimentally.

## Determination of Articular Geometry

Two models can be applied for the determination of articular geometry, both based on stereophotogrammetry (Huiskes et al. 1985; Meijer et al.

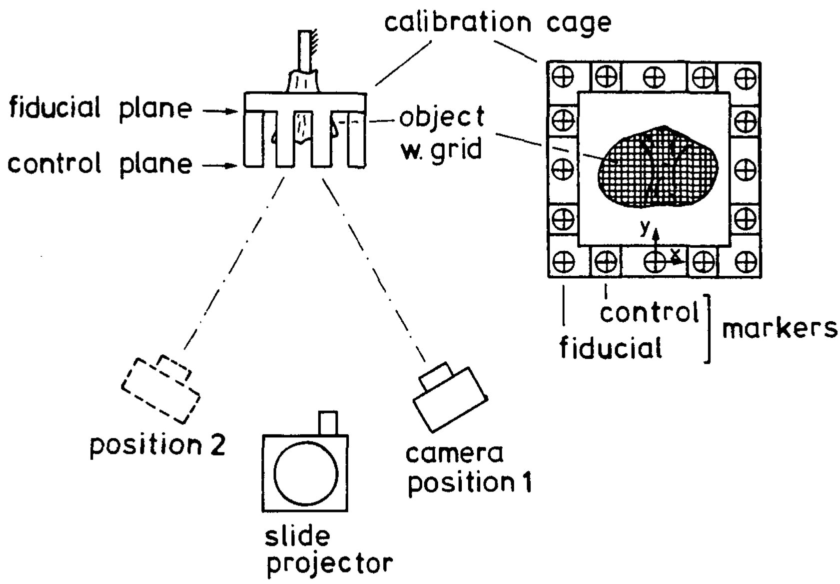


FIGURE 3: Laboratory set-up for the stereophotogrammetric measurements of joint-surface shape on the left (top view), and calibration cage with object (tibia) on the right. (Reproduced from Huiskes et al. (1985), J. Biomechanics, Vol. 18, No. 8, p. 560.)

1989). The first method (Huiskes et al. 1985) uses a set of two technical cameras (or two subsequent camera positions), a slide projector and a calibration cage (Figure 3). The slide projector projects a regular grid on the surface to be measured, of which the intersections are considered as landmarks. The calibration cage contains fiducial and control markers, of which the coordinates are known *a priori*. The images of the calibration markers and the surface landmarks are digitized from both photographs, and their spatial positions reconstructed using a stereophotogrammetric computer program (Selvik 1974).

The mathematical reconstruction assumes that the fiducial markers lie in an ideally flat plane, and that in the photographic imaging procedure all rays pass undistorted through the camera station (central projection). Neither of these requirements is fulfilled exactly, hence reconstruction errors are made. Additional errors occur in the digitization procedure of the photographs. The stochastic errors are minimized by applying optimization techniques to redundant systems of fiducial and control markers.

The digitizer used (ARISTOMAT 104M) has an experimentally verified precision of 20 $\mu$m (S.E.). Accuracy and precision tests carried out with the method (Huiskes et al. 1985) showed that the surface

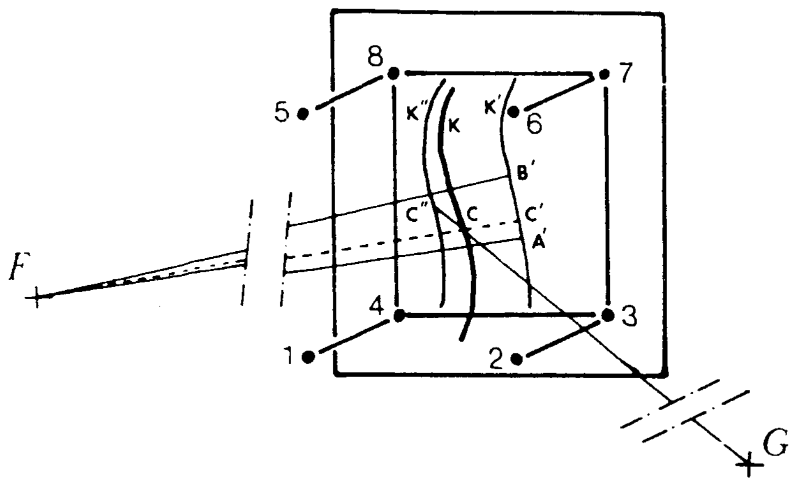


FIGURE 4: Schematic representation of the Stereophotogrammetric Curve Reconstruction (SCR) method. Points 1 to 8 represent landmarks of the calibration cage; F and G are camera stations, imaging curve K as K' and K", respectively. Point C is found as the intersection between line GC" and plane FA'B'. (Reproduced from Meijer et al. (1989), J. Biomechanics, Vol. 22, No. 2, p. 178.)

coordinates of the knee joint can be determined with an accuracy of 0.14 to 0.25 mm (95% confidence interval).

The second method, developed recently (Meijer et al. 1989), is called Stereophotogrammetric Curve Reconstruction (SCR). The principle of the method is depicted in Figure 4. In stead of a grid with landmarks, lines are projected or drawn on the surface to be measured. Each projected curve k is imaged on a stereo pair of photographs (images k' and k"), together with the fiducial and control markers of the calibration cage. These landmarks fulfill the same role as in the procedure described above. The digitization procedure of the photographs now proceeds without identifying the images of the same point on both photographs, but by digitizing the imaged curves k' and k" separately in an arbitrary fashion. For every point C" on k", the reconstruction program determines two points A' and B' on k' with the property that the original point C on k must be located between the original points A and B on k. The position of C is then determined by reconstructing the intersection of the line G-C" (G being one camera station) and the plane F-A'-B' (F being the other camera station). The reconstructed position is an approximation of which the accuracy depends on the curvature of the curve k. The accuracy of the approximation can be improved by increasing the sampling density of the curve digitization procedure. The reconstruction procedure is ill-conditioned when k' and the line G-F tend to co-planarity. Errors can be reduced, in this case, by making multiple stereophotographs.

Error analyses carried out with this system (Meijer et al. 1989) indicated a maximal systematic reconstruction error of 20 $\mu$m. The advantages of this system over the previous one are the faster data-acquisition procedure and the variable sample density, useful if high curvature gradients occur over the surface.

When the articular surface points are determined for femur and tibia, with either of the two methods described above, the surfaces are mathematically described per condyle by surface polynomials, using a least-squares fit to the original data points. For the tibial surfaces, medial and lateral, the polynomials are expressed in Cartesian coordinates of the form $z=z(x,y)$. For the femoral condyles, the polynomials are expressed in spherical coordinates originating from the center of the optimally fitted sphere through the data points, i.e. $R=R(\alpha,\beta)$, in which R is the radius and $\alpha$ and $\beta$ are the two independent spherical angles.

## Variation of Tibial Surface Shape

The purpose of this analysis was to evaluate the effects of tibial surface representation in the model on the passive motion characteristics of the joint. The surface shapes of the femoral and tibial condyles of a knee-joint specimen were measured with the SCR method mentioned above. The measured data points were approximated by polynomials of degree 6 to 7. This same knee specimen was used earlier for extensive experimental evaluations of passive motion characteristics (Blankevoort et al. 1988). The ligament insertions were marked with tantalum pellets, and their positions determined using Roentgen-stereophotogrammetry (Selvik 1974). The Anterior Cruciate Ligament (ACL) and the Posterior Cruciate Ligament (PCL) were described by two line elements each; the Lateral Collateral Ligament (LCL) and the Medial Collateral Ligament (MCL) were described by three line elements each, and the deep fibres of the MCL by two line elements (MCL-c). The model is depicted in Figure 5. The stiffness parameters k and $\varepsilon_1$ for the line elements were derived from experimental data of Butler et al. (1986) and Danylchuk et al. (1975). The zero-load lengths $L_0$ for all line elements were determined in a numerical optimization procedure, subject to the requirement that the experimental passive motion characteristics of the knee-joint specimen are equal to the ones predicted by the model (Blankevoort and Huiskes 1990).

Articular contact was modeled with the linear contact model (7), using a cartilage thickness of 2 mm (Walker and Hajek 1972; Roth 1977), an elastic modulus of 5 MPa (Mow et al. 1982) and a Poisson's ratio of 0.45.

Flexion motions along the envelope of passive knee-joint motion

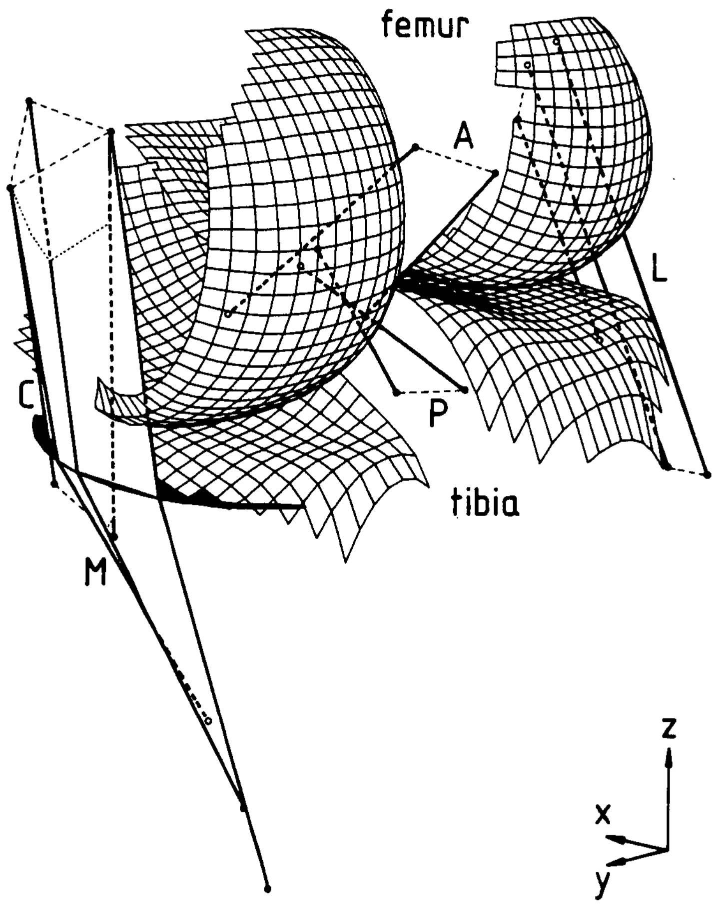


FIGURE 5: Graphic representation of the knee-joint model, showing the femoral condyles, tibial plateaus, and ligament line-elements of anterior (A) and posterior (P) cruciates, lateral (L) and medial (M) collaterals, and medial capsule (C). The medial structures have ligament/bone interaction accounted for.

(Blankevoort et al. 1988) were simulated in the model, by applying flexion as the prescribed kinematic variable, in the presence of a 3 Nm internal rotation torque and a subsequent 3 Nm external rotation torque. In addition, a 150 N axial force was applied in order to prevent the condyles from lifting and loosing contact.

The simulated tests were repeated for a different tibial-surface shape (Figure 6), a linear polynomial fit of the same original surface data points (hence two flat planes, with oblique orientations relative to the horizontal plane).

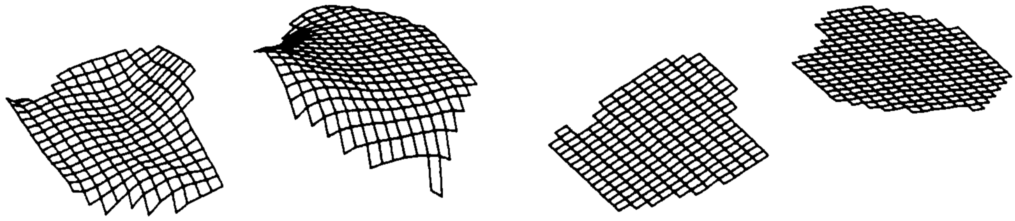

FIGURE 6: The two different descriptions of the tibial surfaces used in the present analyses: a. curved, realistic model, using high-degree polynomials (degree 7 lateral and degree 6 medial), and b. plane fit of the surface data points.

## Surface/Ligament Interactions

The second simulation was meant to study mechanical interactions between the ligaments and the articular surfaces in resisting rotational torques (Blankevoort and Huiskes 1989). Similar characteristics for the model as described above were applied. The tibial (and femoral) surfaces were approximated with high degree polynomials. The flexion angle was fixed (prescribed) at 20 degrees, while prescribing, subsequently, internal rotation and external rotation from 0 to 27.5 degrees, increasing in small steps. All other degrees of freedom (varus/valgus rotation and three translations) were left free, and no other loads were applied. After each step, the ligament forces and the articular contact forces were determined. The ligament and articular forces together equilibrate the external torque, required to realize the axial rotation. In each position the total contributions of the ligaments and of the contact forces to the reaction torque were determined separately, by adding the contribution of each force, as indicated in Figure 7.

This analysis in fact simulates an experiment carried out by Ahmed et al. (1987) with knee-joint specimens, measuring ligament forces with buckle transducers. Other than in the experimental study, the present simulation can also determine contact forces.

# Results

## Variation of Tibial Surface Shape

Figure 8 shows the calculated motion pathways along 'the envelopes of motion', in internal and external rotation, as function of flexion. The results for the plane and the curved tibial plateaus are shown together with the experimental findings (Blankevoort et al. 1988).

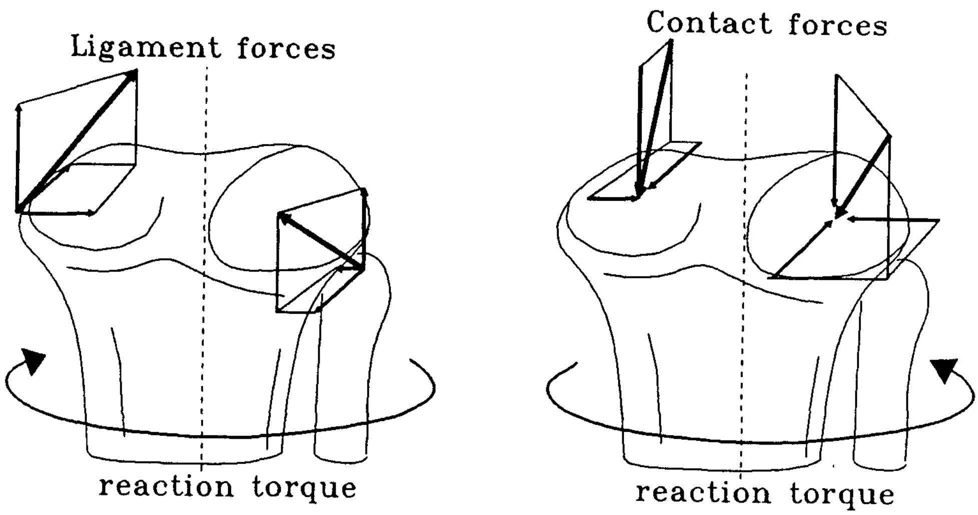


FIGURE 7: The contributions of the ligaments and the contact forces to the total reaction torque in each rotational position is determined by calculating and summing the contributions of the horizontal components of each ligament force (a) and those of each contact force (b).

The curved surface representation yields an excellent approximation of the experimental axial rotation characteristics as function of flexion. The experiments also showed varus/valgus rotations of about zero to plus 2 degrees during the external motion pathway, and about zero to minus 3 degrees during the internal motion pathway. These rotations were also reproduced in the simulation. The relative translations of the bones in AP, medial/lateral and proximal/distal directions found in the experiments were also reproduced in the model simulation with good accuracy, except for AP-translation during the internally rotated motion pathway from zero to about 60 degrees of flexion. In this trajectory the model predicts the femur to be located about 3 to 5 mm more anteriorly relative to the tibia than it was during the experiment. This deviation can be reduced by changing the zero-force lengths ($L_0$) of the line elements, however with the penalty of a somewhat less accurate internal/external rotation position (Blankevoort and Huiskes 1990).

The results of the simulation with the flat-plane representation for the tibial surfaces are clearly less accurate relative to the experimental findings. From zero to about 50 degrees flexion, the internal-rotation laxity is about 3 degrees too high, and the external-rotation laxity up to about 4 degrees too low (Figure 8). After 50 degrees of flexion the internal-rotation laxity reduces progressively, which is not seen in the

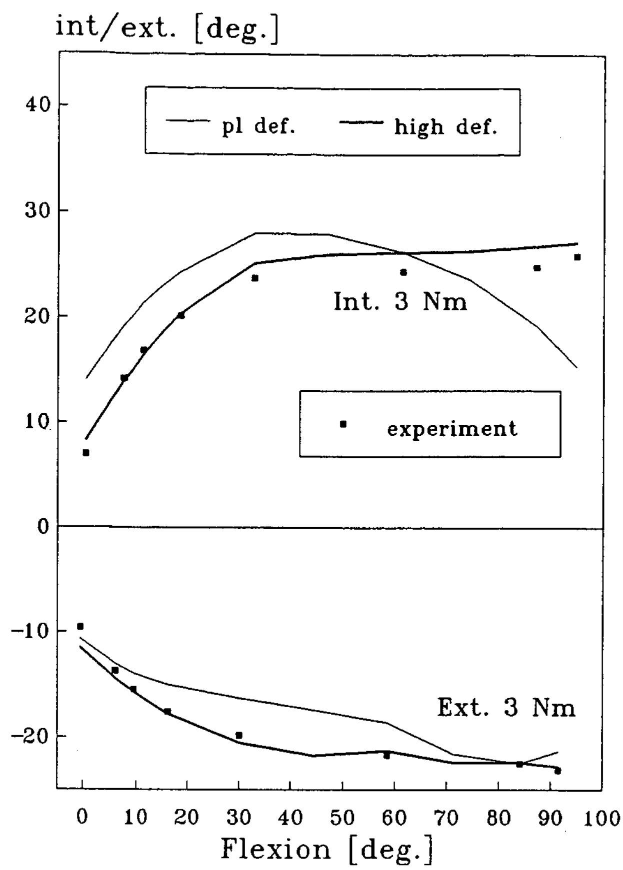


FIGURE 8: Axial rotation as function of flexion for the internal and external envelopes of motion as measured experimentally on a knee-joint specimen and as determined with the knee-joint model for that same specimen, using the realistic, curved representation of the tibial plateaus (high degree polynomial/deformable surface = high def.) and using the plane approximation of the same data point (pl. def.); compare also Figure 6.

experimental results, nor in the curved-surface prediction (Figure 8). Varus/valgus rotation during the internally-rotated motion pathway in particular is not very well predicted. Relative translations follow similar trends as compared to the curved-surface representation, but the values deviate further from the experimental ones. Relative to the curved-surface model, the plane-surface model predicts the femur to be on the average of about 4 mm too much anteriorly and medially, relatively to the tibia, during both motion pathways. It is also continuously about 2 mm more proximally in this case.

It can be concluded that the predictions of passive motion characteristics from the curved-surface approximation are excellent, relative to the experimental findings of the knee-joint specimen simulated. The plane-surface approximation of the tibia gives much less satisfactory results, but when considering the trends relative to the experimental findings, the predictions are still reasonable. The only principle and substantial difference in this case is the reduction of

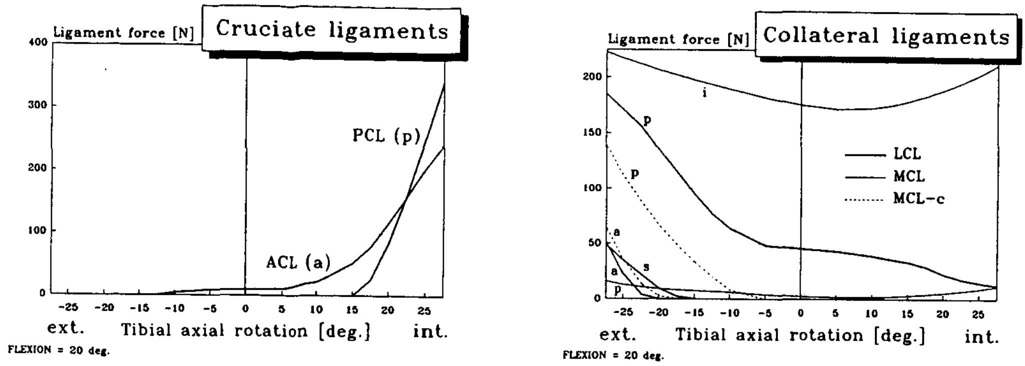


FIGURE 9: Ligament forces found in the simulated-rotation test for the knee in 20 degrees of flexion. (a) Cruciate ligaments (ACL and PCL) are active particularly in internal rotation, (b) collateral ligaments (MCL and PCL) and medial capsule (MCL-c) particularly in external rotation (a=anterior, p=posterior, i=intermediate, s=superior line elements of the ligament concerned).

internal-rotation laxity beyond about 50 degrees of knee flexion, which is not found in the experiments, nor in the curved-surface model prediction. It must be noted, when comparing the predictions, that the numerical optimization procedure for the assessment of the zero-force ligament lengths was based on the curved-surface representation.

## Surface/Ligament Interactions

The results of the axial-rotation simulations are presented in Figures 9 and 10. Figure 9.a shows the forces in the line elements representing the cruciate ligaments as functions of axial rotation, Figure 9.b shows those in the line elements representing the collateral ligaments. Evidently, the ACL and the PCL resist internal rotation only, whereas the MCL and the LCL resist predominantly external rotation. These results are in general agreement with those found experimentally by Ahmed et al. (1987).

The total reaction torque to the axial rotations is shown in Figure 10, subdivided in the part contributed by the ligaments, and the part directly contributed by the articular contact forces. It should be noted that friction at the contact location is neglected, hence the

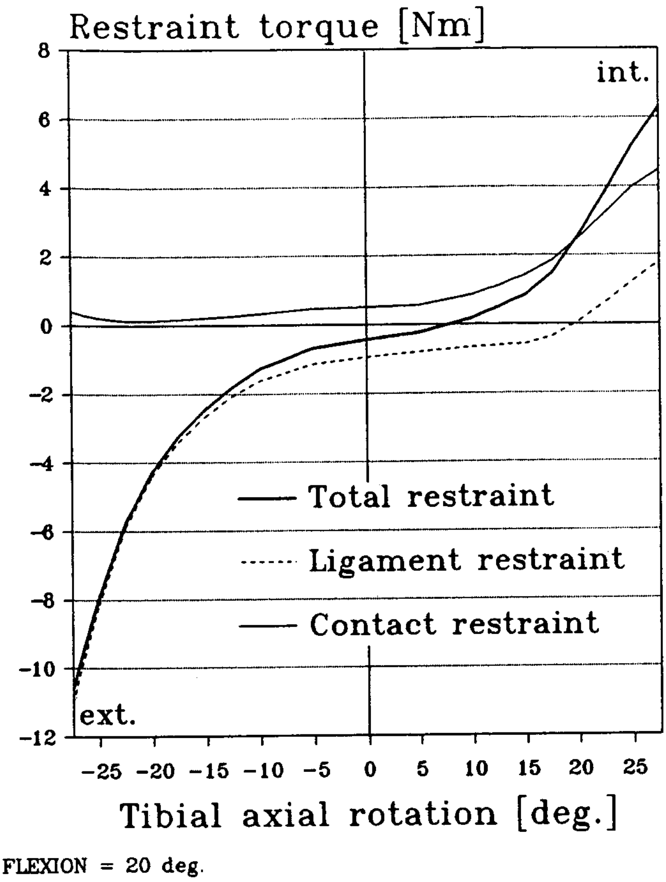


FIGURE 10: Total reaction torque found during the simulated rotation test, the contribution of the ligaments and the direct contribution of the articular contact forces.

contribution is purely an effect of the obliqueness of the articular contact forces, generating a horizontal force component (compare Figure 7.b), and hence of the inclination and the curvature of the tibial plateaus. Particularly in internal rotation, the contribution of the contact forces to the reaction torque is significant. The articular contact contribution is not present in external rotation.

# Discussion

The mathematical knee-joint model presently used, features precise 3-D descriptions of the femoral condyles and tibial plateaus, nonlinear line elements to represent the ligaments, and deformable articular contact, assuming thin-layer, linear-elastic, strain-hardening conditions. Although still crude as compared to the complex reality, it was shown that it can accurately match the passive motion characteristics of a particular knee joint specimen. For this purpose, the joint surfaces of the specimen and the ligament insertion locations were measured. The articular contact parameters were estimated based on literature information. Although the linear cartilage assumption is not adequate to model the bi-phasic behavior of this material (Mak et al. 1987), it seems sufficient for the present purpose. It was found, for example, that an increase of the cartilage elastic modulus from 5 to 10 MPa in the model did not dramatically affect the passive motion characteristics, nor did a change from the linear (7) to the strain-hardening (8) contact condition (Blankevoort et al. 1990). The ligament properties were partly taken from the literature, partly established by an optimization procedure subject to equal passive motion characteristics in the model and in the specimen.

The model can be considered as operational, and can be used to untwine the complex relationships illustrated in Figure 1 in order to develop a better understanding of knee-joint mechanics. The model can be particularly helpful to explain, enhance, and generalize experimental findings, to determine quantities such as articular contact forces which are difficult to measure experimentally, and to develop guidelines for reconstructive procedures and artificial-joint designs.

As the schematic model of Figure 1 indicates, the articular surfaces and the ligaments in fact determine the passive motion characteristics. The effects of individual ligaments have been studied by sequential-cutting experiments (e.g. Butler et al. 1980), ligament length (Wang et al. 1973; Trent et al. 1976; Van Dijk et al. 1979; Arms et al. 1983; Huiskes et al. 1984) and ligament force measurements (e.g. Ahmed et al. 1987). Where the effects of ligament properties in a generic sense are concerned, mathematical models have been used to estimate the effects of stiffness (Wismans et al. 1980; Blankevoort and Huiskes 1987a; Essinger et al. 1990), and the effects of ligament insertion locations (Hefzy and Grood 1986a; Blankevoort and Huiskes 1987b; Sidles et al. 1988). It was found that the passive motion characteristics are rather sensitive to these properties. Very little is known, however, about the effects in a generic sense of the articular surface geometry.

The present analyses confirm that the articular surface geometry and the ligament properties act in concert in determining the motion characteristics of the joint. This is most clearly demonstrated in the mechanism behind the axial-rotation simulation: when moved towards internal rotation, the cruciate ligaments increase and the collateral ligaments decrease in length, due to their particular oblique orientations relative to the tibial axis. Hence, the cruciates in particular resist this motion. In addition, however, due to the inclinations of the tibial plateaus, the tibia screws out, resulting in additional tensioning of the ligaments, hence additional resistance against rotation. Again due to the tibial plateau inclinations, however, the horizontal components of the articular contact forces also contribute *directly* to the rotational reaction torque. Hence, in internal rotation, the reaction torque is built up in three parts: direct cruciate restraint, enhanced restraint due to ligament/articular surface interaction and direct surface restraint. In external rotation the resistance is left to the direct restraints of the collateral ligaments.

The presence of an articular rotation restraint in the knee (in both internal and external rotation!) was hypothesized by Goodfellow and O'Connor (1978). Ahmed et al. (1987) concluded from their experimental assessment of ligament forces, that an additional (unknown) internal rotation restraint must exist, because the reaction torque did not match the applied torque. The present analysis hence partly confirms (internal rotation) and partly rejects (external rotation) the hypothesis of Goodfellow and O'Connor (1978) and presents the unknown restraint which Ahmed et al. (1987) were looking for.

In earlier analyses (Blankevoort and Huiskes 1988) it was shown that these mechanisms could also be demonstrated when the tibial plateaus were modelled as flat planes, albeit with the correct 3-D inclinations relative to the horizontal plane. Hence, important for these mechanisms as a quality of the joint are particularly the 3-D inclinations of the tibial surfaces. The actual curvature distributions of the surfaces then have a second-order effect on the actual magnitudes of the relevant mechanical variables.

A similar conclusion results from the first analysis described in this chapter. Assuming the tibial surfaces as flat planes in the model produces reasonable results in a qualitative sense relative to the passive motion characteristics of the real specimen. Taking the actual curvature of the plateaus into account produces second-order improvements for the mechanical variables. Only when the joint moves in internal rotation for flexion beyond 50 degrees, the plane-surface approximation does yield principle deficiencies by progressively reducing axial rotational laxity. This is due to the fact that in internal rotation the lateral femoral condyle slides down on the posterior slope of the lateral tibial plateau, which is not accounted for in the flat-plane description.

Although the geometries of the femoral condyles were not varied in the present study, earlier analyses (Blankevoort and Huiskes 1987a) have shown that reasonable approximations of the motion characteristics can be produced by the model if both femoral condyles are approximated by spheres. The spherical nature of these condyles was suggested by Kurosawa et al. (1985). For a more accurate simulation of the characteristics, however, a realistic 3-D surface description is needed. Nevertheless, our experience indicates that the passive motion characteristics are not very sensitive to small deviations of the femoral surface description. Or, in other words, tibial geometry (particularly inclination) is more important than femoral geometry.

## Acknowledgements

This research was sponsored in part by the Netherlands Organization of Research (NWO/MEDIGON), Grant Nr. 90-90.

# References

Ahmed AM, Burke DL: In-vitro measurement of static pressure distribution in synovial joints - Part I: tibial surface of the knee. J Biomech Engng 1983;105:216-224.

Ahmed AM, Hyder A, Burke DL, Chan KH: In-vitro ligament tension pattern in the flexed knee in passive loading. J Orthop Res 1987;5:217-230.

Andriacchi TP, Mikosz RP, Hampton SJ, Galante JO: Model studies of the stiffness characteristics of the human knee-joint. J Biomech 1983;16:23-29.

Arms SW, Boyle J, Johnson R, Pope M: Strain measurements in the medial collateral ligament of the human knee: an autopsy study. J Biomech 1983;16:491-496.

Blankevoort L, Huiskes R, Lange A de: An in-vitro study of the passive kinematic behavior of the human knee-joint, in Spilker RL (ed): 1984 Advances in Bioengineering. New York, The American Society of Mechanical Engineers, 1984, pp 57-58.

Blankevoort L, Huiskes R: Mathematical simulations of passive knee joint motions, in Bergmann G, Kölbel R, Rohlmann A (eds): Biomechanics: Basic and Applied Research. Dordrecht, Martinus Nijhoff, 1987a, pp 285-290.

Blankevoort L, Huiskes R: The effects of ACL substitute location on knee joint motion and cruciate ligament strains. Orthop Transact 1987b;11(2):350.

Blankevoort L, Huiskes R: The interaction between articular geometry and cruciate ligament function in the knee joint. Trans. 6th Meeting of the European Society of Biomechanics, Bristol, UK, 1988: 1C.

Blankevoort L, Huiskes R, Lange A de: The envelope of passive knee joint motion. J Biomech 1988;21:705-720.

Blankevoort L, Huiskes R: An alternative rotation restraint in the knee joint. Orthop Transact 1989;13(2):257.

Blankevoort L, Kuiper JH, Huiskes R, Grootenboer HJ: An analysis of articular contact in a three-dimensional model of the knee. J Biomech 1990, (submitted).

Blankevoort L, Huiskes R: Parametric validation of a 3-D knee joint model. 7th Meeting of the European Society of Biomechanics, Aarhus, Denmark, 1990.

Butler DL, Kay MD, Stouffer DC: Comparison of material properties in fascicle-bone units from human patellar tendon and knee ligaments. J Biomech 1986;19:425-432.

Butler DL, Noyes FR, Grood ES: Ligamentous restraints to anterior-posterior drawer in the human knee. J Bone Jt Surg 1980;62-A:259-270.

Crowninshield R, Pope MH, Johnson RJ: An analytical model of the knee. J Biomech 1976;9:397-405.

Danylchuk K: Studies on the morphometric and biomechanical characteristics of ligaments of the knee joint, MSc thesis. Unversity of Western Ontario, London, Ontario, Canada, 1975.

Dijk R van, Huiskes R, Selvik G: Roentgenstereophotogrammetric methods for the evaluation of the three-dimensional kinematic behaviour and cruciate ligament length patterns of the human knee joint. J Biomech 1979;12:727-731.

Dijk R van: The behavior of the cruciate ligaments in the human knee. Dissertation. University of Nijmegen, Nijmegen, The Netherlands, 1983.

Edixhoven P, Huiskes R, Graaf R de: Anteroposterior drawer measurements in the knee using an instrumented test device. Clin Orthop 1989;247:232-242.

Essinger JR, Leyvraz PF, Heegard JH, Robertson DD: A mathematical model for the evaluation of the behaviour during flexion of condylar-type knee prostheses. J Biomech 1989;22:1229-1241.

Fukubayashi T, Torzilli PA, Sherman MF, Warren RF: An in vitro biomechanical evaluation of anterior-posterior motion of the knee. J Bone Jt Surg 1982;64A:258-264.

Goodfellow J, O'Connor J: The mechanics of the knee and prosthesis design. J Bone Jt Surg 1978;60-B:358-369.

Grood ES, Suntay WJ: A joint coordinate system for the clinical description of three-dimensional motions: applications to the knee. J Biomech Eng 1983;105:136-144.

Hefzy MS, Grood ES: Sensitivity of insertion locations on length patterns of anterior cruciate ligament fibers. J Biomech Eng 1986;108:73-82.

Huiskes R, Blankevoort L, Dijk R van, Lange A de, Rens ThJG van: Ligament Deformation Patterns in Passive Knee-Joint Motions, in Spilker RL (ed): 1984 Advances in Bioengineering. New York, The Am Soc Mech Engrs, 1984, pp. 53-54.
Huiskes R, Kremers J, Lange A de, Selvik G, Woltring HJ, Rens ThJG van: An analytical stereo-photogrammetric method to determine the 3-D geometry of articular surfaces. J Biomech 1985; 18:559-570.
Kalker JJ: A course on contact mechanics. Delft University of Technology, Delft, The Netherlands, 1985.
Kurosawa H, Walker PS, Abe S, Garg A, Hunter T: Geometry and motion of the knee for implant and orthotic design. J Biomech 1985;18:487-499.
Mak AF, Lai WM, Mow VC: Biphasic indentation of articular cartilage - I. theoretical analysis. J Biomech 1987;20:703-714.
Markolf KL, Mensch JS, Amstutz HC: Stiffness and laxity of the knee - The contributions of the supporting structures. J Bone Jt Surg 1976;58A:583-593.
Meijer RCMB, Huiskes R, Kauer JMG: A stereophotogrammetric method for measurements of ligament structure. J Biomech 1989;22:177-184.
Mow VC, Lai WM, Holmes MH: Advanced theoretical and experimental techniques in cartilage research, in Huiskes R, Campen DH van, Wijn JR de (eds): Biomechanics: principles and applications . The Hague, Martinus Nijhoff Publishers, 1982, pp 47-74.
Roth V: Two problems in articular biomechanics: I. Finite element simulation for contact problems of articulations, II. Age dependent tensile properties, PhD thesis. Rensselaer Polytechnic Institute, Troy NY, 1977.
Selvik G: A roentgenstereophotogrammetric method for the study of the kinematics of the skeletal system. Dissertation. University of Lund, Sweden, 1974.
Sidles JA, Larson RV, Garbini JL, Downey DJ, Matsen FA: III Ligament length relationships in the moving knee. J Orthop Res 1988;6:593-610.
Trent PS, Walker PS, Wolf B: Ligament length patterns, strength and rotational axes of the knee joint. Clin Orthop Rel Res 1976;117:263-270.
Walker PS, Hajek JV: The load-bearing area in the knee joint. J Biomech 1972;5:581-589.
Wang CJ, Walker PS, Wolf B: The effects of flexion and rotation on the length patterns of the ligaments of the knee. J Biomech 1973;6:587-596.
Wismans J, Veldpaus F, Janssen J, Huson A, Struben P: A three-dimensional mathematical model of the knee-joint. J Biomech 1980;13:677-685.
Woo SLY, Gomez MA, Seguchi Y, Endo CM, Akeson WH: Measurements of mechanical properties of ligament substance from a bone-ligament-bone preparation. J Orthop Res 1983; Vol 1: pp 22-29.